JOURNAL OF GEOPHYSICAL RESEARCH, VOL. 100, NO. C1, PAGES 921–936, JANUARY 15, 1995

Application of a mixed layer model to the inner Newfoundland shelf

T. Mathieu and B. deYoung

Department of Physics and Ocean Sciences Centre, Memorial University of Newfoundland, St. John's, Newfoundland, Canada

Abstract. A mixed layer model is developed and applied based upon the model of Price, Weller, and Pinkel (Price et al., 1986). The new model includes diffusion, adds salinity to the calculation of density, and permits the assimilation of observed monthly mean salinity profiles. A simulation over a 2 year period on the inner part of the Newfoundland shelf shows that the new model performs well, much better than the previous model. The assimilation of salinity has relatively little effect, but the model results are sensitive to the parameterization of the vertical diffusivity. The best results are found for the case where the diffusivity is dependent upon N^2; hence there is an indirect dependence on the salinity profile. The heat content of the model is simulated well except in late summer when there is too much heat in the model.

1. Introduction

In this paper we shall investigate the application of a bulk one-dimensional model which is an extension of the *Price et al.* [1986] model, commonly referred to as the Price-Weller-Pinkel (PWP) model. The modified model includes diffusion which will smooth the density profile over the depth and will also deepen the mixed layer (ML). We include salinity in the calculation of density because the model is applied at a high latitude. We also assimilate salinity to account for the horizontal advection of fresh and salt water. Our goal is to develop a model to simulate the primary production cycle in coastal waters, during the spring bloom period [*Marra and Ho*, 1993] and the summer upwelling period. We are encouraged to apply a one-dimensional model to the inner part of the Newfoundland shelf (Figure 1) because of the work of *Petrie et al.* [1991], who showed that a one-dimensional diffusion model with a constant diffusivity could fit the seasonal profile of temperature, suggesting that advection of heat is unimportant there. We define the inner part of the shelf as that region under the influence of the inshore branch of the Labrador Current [*Petrie et al.*, 1991], located within 50-100 km of the coastline.

The two primary processes which control the depth of the mixed layer are the heat balance which induces warming at the surface and the wind stress which produces kinetic energy in the mixed layer [*Krauss and Turner*, 1967; *Denman*, 1973; *Niiler and Krauss*, 1977]. The first phenomenon is dependent upon the heat fluxes: latent, sensible, incoming and outgoing long wave, and the short wave flux, all of which exhibit strong seasonal variations [*Häkkinen and Cavalieri*, 1989]. The mixing, induced by the wind stress at the sea surface, is balanced by energy dissipation, an increase of kinetic energy in the mixed layer, and an energy flux across the pycnocline [*Largier*, 1991]. During the summers, in the absence of wind stress, the heating at the sea surface induces strong stratification of the upper water column which results in a shallowing of the mixed layer. Momentum transfer at the surface, during a wind event, increases the turbulence in the upper water column, thereby homogenizing it [*Niiler*, 1975]. Other kinetic energy sources such as internal waves are generally ignored. What are the best ways to parameterize these processes?

Several different models have been developed to simulate the evolution of the mixed layer [*Niiler and Kraus*, 1977]. Differential models solve the basic equations by using a turbulence closure scheme which involves diffusion between the different layers [*Yamada and Mellor*, 1974; *Nihoul*, 1984]. On the other hand, bulk models integrate differential equations over the whole mixed layer, which results in a homogeneous upper layer [*Krauss and Turner*, 1967; *Price et al.*, 1978; *Price et al.*, 1986]. In these latter models, eddy diffusivity is eliminated and deepening of the mixed layer induces an instantaneous mixing of mass, heat, and salt through the layer, generating a sharp jump in density at the base of the upper layer. Both types of model (differential and bulk) have been used to reproduce the variation of the mixed layer depth. *Martin* [1985] provided a good comparison of several different models. He showed the importance of optical parameters of the seawater and of the ambient diffusivity for differential models. He also pointed out the advantages of long timescale simulations. For long-timescale studies (up to 3 years), *Gaspar* [1988] showed that the classical model of *Niiler and*

Paper number 94JC01435.
0148-0227/95/94JC-01435$05.00

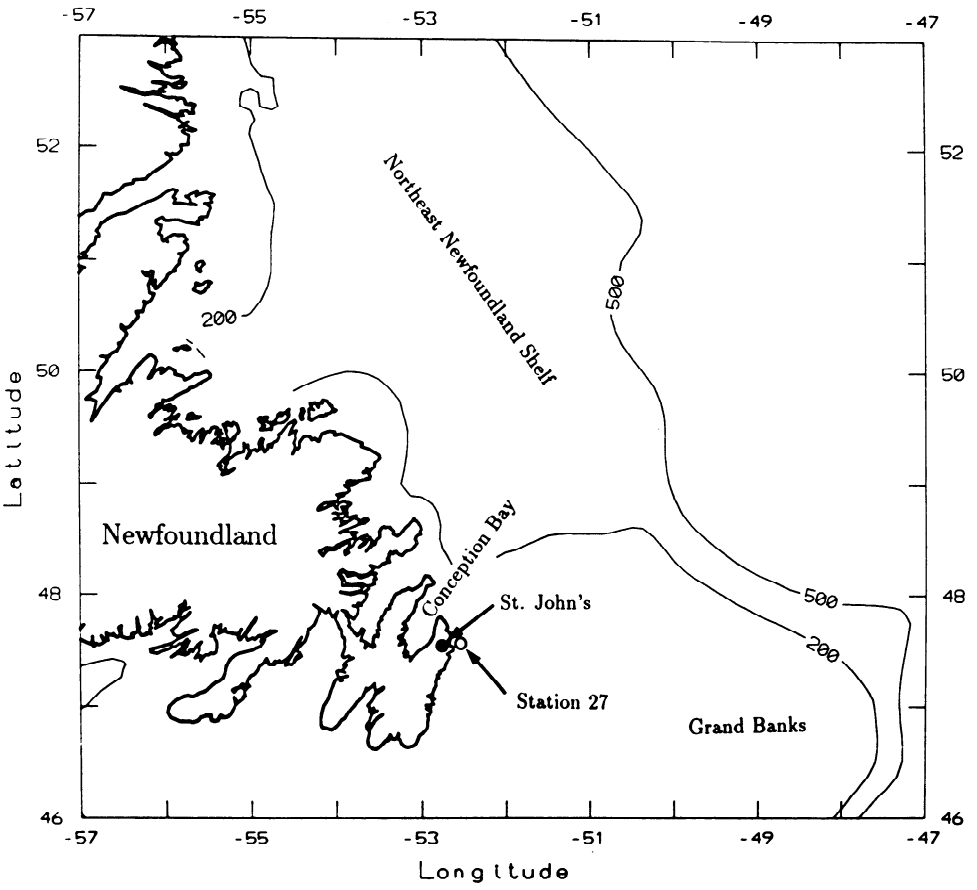

Figure 1. Study area map with location of Conception Bay and Station 27, located 5 km offshore St. John's. Contours show the bottom depth in meters.

Krauss [1977] produced sea surface temperature (SST) with some systematic errors during the summer (overestimated) and in autumn (underestimated). He correlated these SST variations to the depth of the mixed layer which was underestimated in summer and overestimated during autumn. *Price et al.* [1986] developed a bulk mixed layer model (PWP) that differed from the conventional models. To avoid the sharp density jump between the mixed layer and the deep layer, they integrated a transition layer using a criterion based upon the gradient Richardson number. Numerical and conceptual simplicity are the principal advantages of the PWP model, advantages which we wish to retain.

In the next section, the model equations and parameterizations of fluxes shall be presented. A brief description of the study area shall be given in section 3 followed by a section on the model results, which shall include some discussion of model parameters. At the end, we shall discuss some of the implications of the model results.

2. Model Description

The model is an integrated model in which the mixed layer (ML) is defined by a constant temperature and salinity. To obtain such a representation, the primitive equations are integrated over the depth of the mixed layer. Beneath the mixed layer, the interface layer allows a smooth transition between the mixed layer and the deep layer. The basic model is the Price-Weller-Pinkel (PWP) model [*Price et al.*, 1986] to which we have made some modifications.

The PWP model was modified to include diffusion because of the need to run the model for long time periods. In its original application, the model was run for only several days [*Price et al.*, 1986]. Diffusion is added to account for physical processes, such as internal waves, not in the original PWP model. The three equations for the conservation of heat, salt, and momentum are described here:

$$\frac{\partial S}{\partial t} = -\frac{\partial E}{\partial z} + \frac{\partial}{\partial z}(\kappa_v \frac{\partial S}{\partial z}) \tag{1}$$

$$\frac{\partial T}{\partial t} = \frac{-1}{\rho_0 c}\frac{\partial Q}{\partial z} + \frac{\partial}{\partial z}(\kappa_v \frac{\partial T}{\partial z}) \tag{2}$$

$$\frac{\partial \mathbf{V}}{\partial t} = -\mathbf{f} \times \mathbf{V} - \frac{1}{\rho_0}\frac{\partial \mathbf{G}}{\partial z} + \frac{\partial}{\partial z}(\kappa_v \frac{\partial \mathbf{V}}{\partial z}) - r\mathbf{V} \tag{3}$$

where T is temperature, S is salinity, $\mathbf{V}$ is velocity, κ_v is eddy diffusivity, $\mathbf{f}$ is the Coriolis vector, Q is the sum of heat fluxes, E is the evaporation minus precipitation,

G is the wind stress, and r the dissipation timescale is 5 days. These equations were integrated over the depth of the mixed layer to obtain a constant salinity, temperature, and velocity in the upper layer.

There are two differences between this model and that of PWP. First, we have explicitly added dissipation to keep the surface velocity from becoming too large. In the PWP model, dissipation came from numerical diffusion; however, we found this to be insufficient for long runs. Second, we have added vertical diffusion, of heat, salt, and momentum. Note that we include a parameterization that has κ_v varying with depth. In the section on parameters, we shall discuss how the parameterization for κ_v was chosen.

The boundary conditions were determined from the usual fluxes at the sea surface. In our simulations (downward direction positive), Q, the net flux, is equal to

$$Q = H + SHW + \delta_r LW_o + \delta_r LW_i + LT \qquad (4)$$

where H is the sensible heat flux computed from the air-sea temperature difference, SHW the incident short wave flux, LT the latent heat flux (both determined according to *Parkinson*, [1979]), LW_o the outgoing long wave radiations computed by

$$LW_o = \sigma T_s^4 \qquad (5)$$

LW_i is the incoming long wave radiations determined by the empirical equation

$$LW_i = \sigma T_a^4 (a + b\sqrt{e})(1 + cN) \qquad (6)$$

where a, b, c are empirical constants, e is vapor pressure, N cloud cover, σ the Stefan Boltzman constant, T temperature, and δ_r the transmittance [*Dera*, 1992]. The short wave radiations (SHW) were obtained from observations at St John's. The downward irradiance is absorbed through the water column using double exponential depth form [*Krauss*, 1972]:

$$I_z = I_0[I_1 exp(-z/\lambda_1) + I_2 exp(-z/\lambda_2)] \qquad (7)$$

in which z is the depth (downward direction positive), the subscripts 1 and 2, respectively, represent the short and long wave components of the incoming solar radiation, and λ_i represents the extinction coefficient of the water for each component. The values of the different parameters used in the equations are provided by *Paulson and Simpson* [1977] and are given in Table 1.

The criteria, used by *Price et al.* [1986], to maintain shear stability was replaced by the usual turbulence kinetic energy parameterization of *Niiler and Krauss* [1977] and *Price et al.* [1978]. This parameterization is shown here as

$$-g\frac{1}{2}W_e h = m_1 \frac{1}{2} h B_0 H(B) + m_2 \frac{1}{2} W_e \triangle \mathbf{V^2} + m_3 \mathbf{U_*^3} \qquad (8)$$

Equation (8) replaces the bulk Richardson number criteria because it partitions kinetic energy in three components: energy release during free convection, energy due to the shear flow of the bottom of the ML, and energy due to the wind stress at the sea surface [*Niiler and Krauss*, 1977]. *Price et al.* [1978] showed a good evolution of the kinetic energy using this formulation. The equation initially used by *Price et al.*, [1986] is strongly dependent on the salinity evolution. We found that there was strong feedback in the model when using the bulk Richardson number formulation which is difficult to apply when vertical stratification becomes weak during the winter months.

Kinetic energy results from the sum of the energy released during free convection, the energy due to the shear flow at the bottom of the ML, and the energy due to the wind stress at the sea surface [*Niiler and Krauss*, 1977]. In these equations, W_e represents the entrainment velocity associated with the layer deepening, g is gravity, h is the depth of the mixed layer, B_0 is the air-sea buoyancy flux (proportional to the temperature and salinity of the mixed layer), and $H(B)$ is a Heaviside function which is equal to 1 when B_0 is positive and equal to 0 when the buoyancy flux is negative [*Price et al.*, 1978]. The three coefficients m_1, m_2, and m_3 are called parameters of energy conversion efficiency, and are considered constant. The density, computed as σ_t using the Unesco equation of state [*Gill*, 1982], depends upon temperature and salinity.

Price determined the mixed layer as a layer with a temperature anomaly up to 0.02°C (or a velocity anomaly of 0.01 m s^{-1}). The density jump across the pycnocline is reduced by the mixing processes which occur in the transition layer. The depth of this layer is

Table 1. Values for the Different Coefficients Used in the Model

	Coefficient	Value	Unit
a	empirical coefficient	0.34	...
b	empirical coefficient	0.05	...
c	empirical coefficient	0.15	...
σ	Stefan-Boltzmann constant	5.668×10^8	$Wm^2\ K^{-4}$
δ_τ	Transmittance coefficient	0.96	...
λ_1	Extinction coefficient of short wave	0.6	m
λ_2	Extinction coefficient of long wave	20	m
I_1	Short wave component of insolation	0.62	...
I_2	Long wave component of insolation	0.48	...

determined by using a criterion based upon the gradient Richardson number:

$$R_g = \frac{g\ \partial\rho/\partial z}{\rho_0\ (\partial V/\partial z)^2} \geq 0.25 \qquad (9)$$

This transition layer induces a smooth evolution of the density over the depth. As long as the value of R_g is lower than the critical value, the mixing processes occur in the transition layer, between the two grid levels that produced this small value. This computation is extended to the previous and next grid levels until the value of R_g is greater than its critical value.

3. Observations and Data

We choose to analyze data from a site on the inner Newfoundland shelf. The Station 27 data cover a 2-year period starting in January 1988. We choose this period because we had additional data from Conception Bay (see Figure 1) during this same period collected as part of the Cold Ocean Productivity Study (COPE) [*deYoung et al.*, 1993a,b]. Station 27 data include temperature and salinity measured at 11 depths (0, 10, 20, 30, 40, 50, 75, 100, 125, 150, and 175 m in 179 m of water). We use these data because they provide a long time series (over 50 years) measure at least once a month. The station is, however, only 5 km offshore St. John's and thus is partially influenced by the coastal response to wind forcing. Initialization profiles of temperature and salinity were taken from a conductivity-temperature-depth (CTD) profile obtained on April 17, 1988, in the center of Conception Bay. Comparisons between observations in Conception Bay and at Station 27 show good agreement during this period down to depths of $\sim$ 175 m, somewhat below the sill depth of the bay.

Temperature and salinity profiles have been collected at Station 27 on at least a monthly basis for almost 50 years. *Petrie et al.* [1991, 1992] have looked at both the annual and the interannual fields for Station 27 (see Figure 1). In their analysis of the annual field they estimated vertical diffusion coefficients by fitting a one-dimensional diffusion model to the data. They showed that for the salinity data, an advective term had to be included; however, no advection was needed to fit the temperature data. There are strong annual cycles in both temperature and salinity at this site, with a maximum in surface temperature and a minimum in salinity in late summer (Figures 2a and 2b). The summer salinity minimum is a result of the melting of sea ice which forms to the north on the shelf and generates a freshwater flux which moves down the shelf [*Mertz et al.*, 1993]. In our analysis, we shall apply a mixed layer model to these data, as a test of the model, and also to further explore the seasonal signal at this site. We are interested in determining the influence of vertical diffusion and also the relative importance of salinity in constraining a mixed layer model for this region. The salinity problem is interesting for two reasons: (1) the importance of salinity in determining density in this subpolar region and (2) the need for including an advective term in the salinity budget for this region [*Petrie et al.*, 1991].

The wind stress at the sea surface is computed following *Large and Pond* [1981]. The wind and flux used for the surface boundary conditions are computed from hourly atmospheric data measured at St. John's (Atmospheric Environment Service, Canada). Figure 3 shows the amplitude of the wind stress and the net surface heat flux for 1989. A strong seasonal signal is apparent in both time series, with large variations apparent at synoptic periods (2-10 days). The model was run at a time step of 1000 s. All the data were interpolated to this time interval. Station 27 data were linearly interpolated over depth to obtain 1 m resolution for the temperature and salinity profiles. To include a diffusion parameterization in our model, we computed N^2 from the interpolated density profiles of Station 27. Monthly averages of N^2 were used to represent the seasonal cycle. The N^2 analysis was based upon the complete data set of Station 27 data, from 1946 to 1992; thus it represents the best estimate of the mean seasonal signal of N^2. Monthly mean data for salinity were obtained in the same way.

4. Numerical Simulations

The vertical resolution of the grid is 1 m. The basic equations (equations (1)-(3)) are integrated for each grid level over the depth. The depth of the mixed layer is determined according to a density jump greater than $1. \times 10^{-4}$ kg m^{-3} between two levels. Once the mixed layer depth is known, temperature, salinity, and velocity are mixed over this upper layer to obtain a homogeneous layer. According to the kinetic energy content (mixed layer) and the criterion used for the Richardson number (transition layer), the mixing processes occur between the bottom of each layer and the level below to satisfy the stability requirement. This mixing will be repeated and extended over the previous and next level until stability in the layers is reached. Diffusion takes place before the determination of the mixed layer depth. This added process allows a distribution of temperature, salinity, and velocity according to the gradient between two levels. The time step chosen for our simulation is 1000 s. The initial temperature and salinity data are taken from a CTD profile obtained April 17, 1988. The total model depth is 160 m. The simulations run from April 17, 1988 (day 108) to April 7, 1990 (day 819). The day count is calculated from January 1, 1988.

Results of the model simulations over 2 years are compared with data collected during the simulation period. The results of several runs are analyzed to determine appropriate parameters for the model. We shall also consider the influence of the integration of different salinity data on the diffusion model results. Runs were conducted with identical atmospheric fluxes and initial data. We tested the sensitivity of the model to the initial conditions and found little dependence.

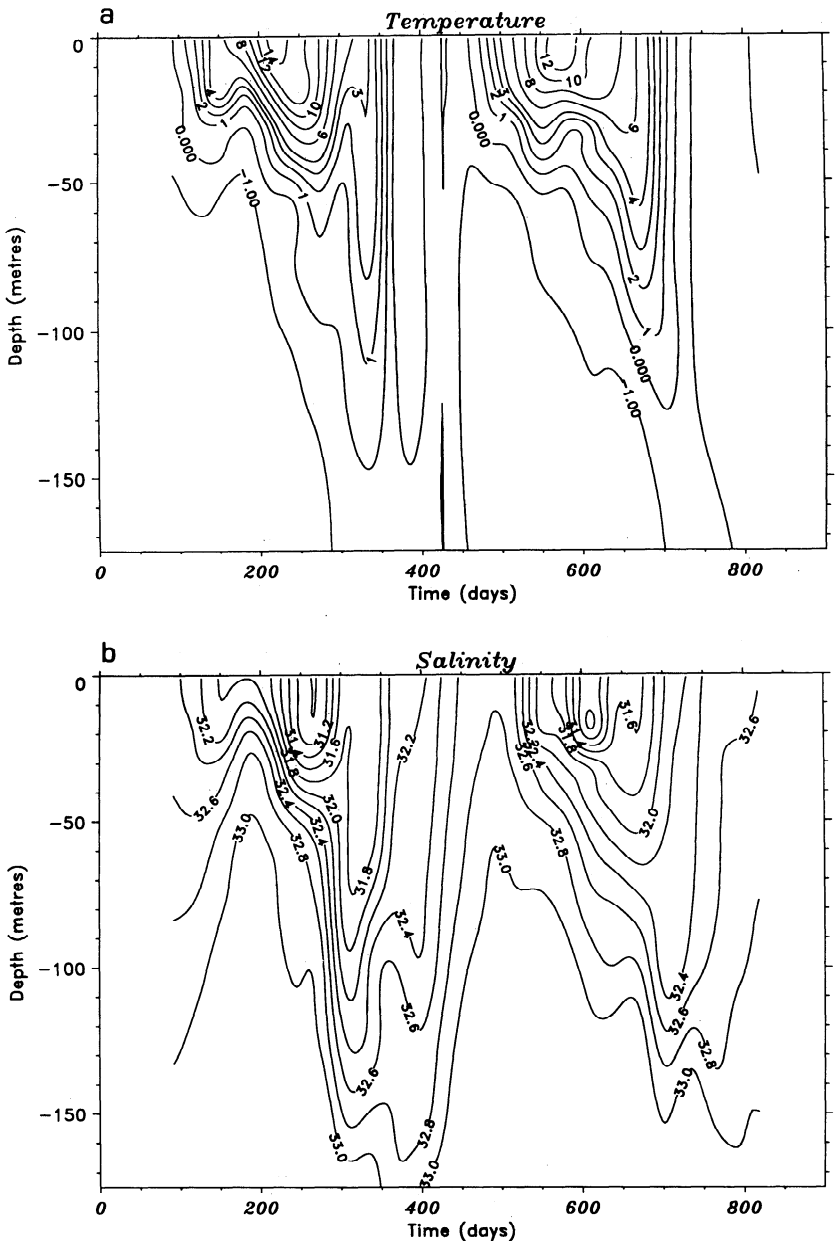

Figure 2. The seasonal evolution of (a) temperature (in degrees Celsius) and (b) salinity at Station 27 during the simulation period, 1988 and 1989. The sampling period for the data, although irregular, is about two weeks. Time is in days from the start of 1988.

4.1. Parameters

Several parameters are necessary in the model runs. The most important for the determination of the mixed layer are the parameters of energy conversion efficiency m_1, m_2, and m_3 used in equation (9). The values of those constants are obtained from *Price et al.* [1978], who investigated the response of their model to combinations of different parameters values. However, we found that a modification of parameter m_3 seems to improve the correlation between data and the model results. The constants used in our model are $m_1 = 0.2$, $m_2 = 0.7$, and $m_3 = 0.5$. The changes made from the original model represent some tuning for the local physical conditions.

It was *Munk and Anderson* [1948] who first suggested a relation between κ_v and the Richardson number. This has been further developed by *Pacanowski and Philander* [1981], who tested a mixing parameterization, suggested by *Robinson* [1966] and *Jones* [1973], also based upon the Richardson number.

$$\kappa_v = \frac{\kappa_0}{(1+\beta Ri)^n} + \kappa_b \tag{10}$$

where Ri is the Richardson number, and κ_0, n, β, and κ_b are all empirical constants. Theoretical support for this approach comes from the work of *Gargett* [1984]. *Umoh* [1992] obtained vertical diffusivities for the northwest Atlantic using a slightly different formu-

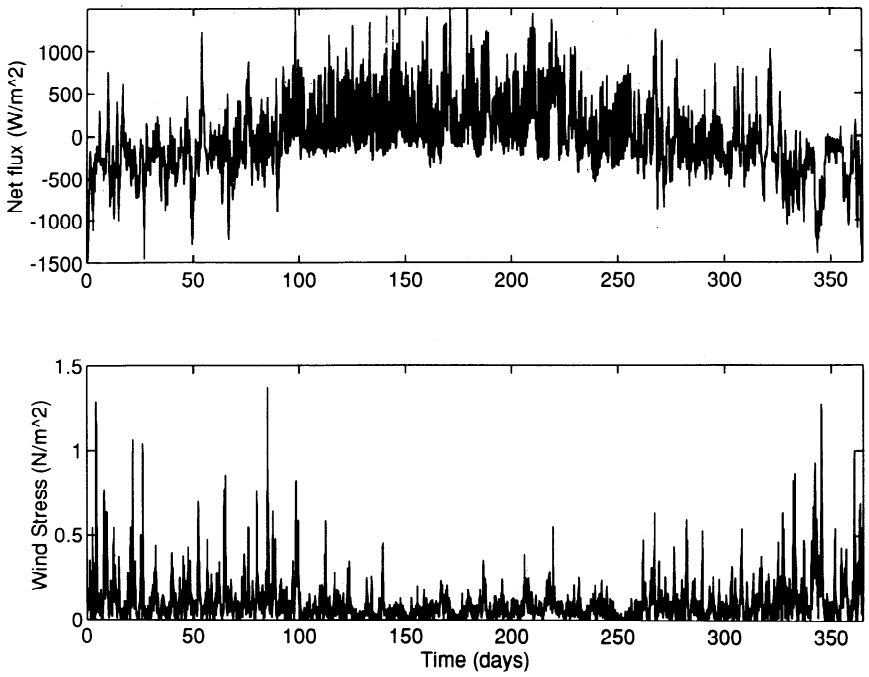

Figure 3. Time series (for 1989) of net surface heat flux, in Watts per square meter, and the amplitude of the wind stress, in Newtons per square meter.

lation, where the dependency of κ_v is on N^2 and not on Ri:

$$\kappa_v = \frac{\kappa_0}{(1+\alpha N^2)} \tag{11}$$

Here N^2 is the Brünt Väisälä frequency, and κ_0 and α are two empirical coefficients. Experimental work has clearly shown that, in coastal waters at least, this relation holds [*Stigebrandt,* 1976; *deYoung and Pond,* 1988]. We did try the approach of *Pacanowski and Philander* [1981] but with little success, perhaps because of the difficulties associated with calculating the vertical profile of the Richardson number in the model. In his analysis, *Umoh* [1992] found a wide range of values for κ_0 and β. We choose values here that are roughly representative and produce profiles of κ_v that have about the same mean as found by *Petrie et al.* [1991] in their analysis of the annual temperature and salinity data.

All the other parameters used in the model, most of them associated with the various flux terms, are shown in Table 1 (section 2).

4.2. Influence of Diffusion

In the first set of runs, we tested the sensitivity of the model results to diffusion. Salinity is used to compute σ_t, but there is no evolution of salinity except from the evaporation minus precipitation term.

4.2.1. No diffusion: $\kappa_0 = \alpha = 0$. For $\kappa_0 = \alpha = 0$, the case is similar to the initial PWP model. Sea surface temperature exceeds 25°C in the summer, with a maximum of 33.2°C in 1988 and a maximum of 32.2°C in 1989 (Figure 4). In the winter, the minimum temperature does not go below 0°C. Comparison with SST data from Station 27 shows an overestimate of ~70% during summer months and ~40% in the winter. The temperature profiles (Figure 5) show, at the beginning of the summer (days 153 and 497), warm SST due to heat in the mixed layer. Without any diffusion, heat is trapped in the upper layer because wind mixing is not energetic enough to mix it downwards. The transition layer has a weak influence on the sharp temperature variation at the bottom of the ML. Similar observations apply to the summer profiles (days 239 and 616), but for these latter the accumulation of heat in the mixed layer is greater and induces a maximum temperature. In the absence of diffusion, there is a downward heat flux over the summer because of weak mixing which occurs at the bottom of the transition layer. Wintertime profiles (days 421 and 762) show a deep mixed layer with a temperature jump of ~1°C at the bottom.

4.2.2. Constant diffusion: $\kappa_0 = 2.\times 10^{-4}\ m^2\ s^{-1}$, $\alpha = 0$. For the constant diffusion case we choose a value of κ_v similar to that found by *Petrie et al.* [1991] in their analysis. For these empirical values, SST evolution is similar to the previous case but with much lower maxima during summer (Figure 4). The constant diffusion over depth results in a heat flux from the mixed layer to the deep layers. This process generates an increase in bottom temperature and a decrease of SST. During winter (days 421 and 762), the upper layer temperature decreases according to the heat loss from ocean to atmosphere until a straight temperature profile is achieved (Figure 5). Then, constant diffusion allows, independently of the ML depth, a removal of heat from the whole water column. However, wintertime heat loss is not sufficient to decrease the temperature of the water column, and winter temperatures are still overestimated. Excess heat stored during the sum-

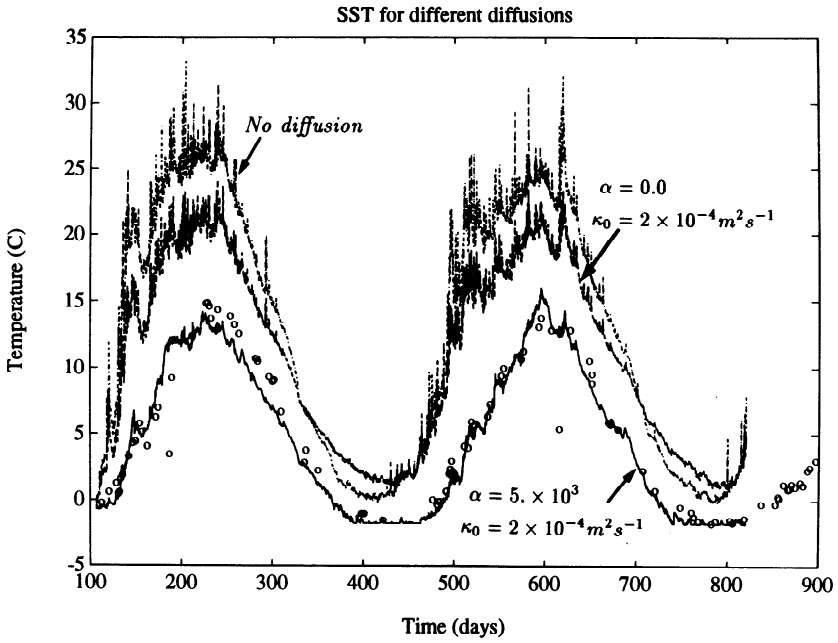

Figure 4. Time evolution of simulated sea surface temperature over the two years for different values of α and k_o in equation (4). The data from Station 27 are shown with open circles. The different diffusion cases are labeled.

mer keeps the winter temperatures from dropping to their observed values. This process results in a higher wintertime SST than the previous case (no diffusion).

4.2.3. Depth dependent diffusion: $\kappa_0 = 2. \times 10^{-4}\ m^2\ s^{-1}$, $\alpha = 5. \times 10^3$. We choose values of the constants in equation (14) based upon the work of *Umoh* [1992], who analyzed temperature data for the northwest Atlantic to determine vertical profiles of diffusivity. The values of κ_0 and α produce a subsurface minimum in κ_v where N^2 is at a maximum, roughly at the base of the mixed layer. We use the monthly mean data to provide the N^2 profile which is used to compute the profile of κ_v. Thus the vertical profile of κ_v is adjusted each month using equation (14) and the observed profile of N^2. From observation of Figure 4, results of this run are well correlated with SST data. At the beginning of each year, modeled SST agrees well with the observations. From the middle of summer 1988 until winter, the model sea surface cools somewhat faster than observed. Profiles at days 153 and 239 (Figure 5) show good correlation between the simulated and observed temperature. However, for both days the water column has too little heat at the surface ($\triangle$ T of $\sim$1°C) and too much in the transition layer. In the winter, the fluxes invert, and the diffusion induces a heat loss from the first 100 m. The bottom heat accumulated during summer is lost slowly because of weak diffusion in the deep layers. The second year of the simulation produced better agreement with observations. However, at the end of the summer of 1989, the cooling still seems too fast in the model, although the discrepancy is less than observed in 1988.

The modeled mixed layer depth is determined where the temperature variation exceeds 0.02°C over 1 m. The mixed layer depth for the data was defined as the depth at which the difference from the SST is greater than 0.2°C. From the data we choose a bulk measurement, so 0.2°C over 10 m is equal to the model evaluation of 0.02°C over 1 m. Figure 6 shows the simulated and observed ML depth for different values of diffusivity. The mixed layer depth obtained from simulations was filtered to remove energy at periods less than 1 day.

4.2.4. Mixed layer depth. The correlation between simulated and observed ML depth is good, particularly at the beginning of summer when shallowing of the mixed layer occurs. The ML simulations can also be related to the SST [*Gaspar*, 1988] as observed in Figure 4. Since the ML is homogeneous for all variables, these are averaged over the layer, and so the upper layer depth can influence the values in the mixed layer. During the summer of 1988, the modeled ML is deeper than observed, although over the season the difference decreases until it is reversed by winter. The mixed layer is observed to reach a depth of 50 m during this period (Figure 6). The shallowing of the upper layer by the beginning of the next summer is due to the greater influence of heating and the decrease of the wind stress at the sea surface during this period. Again, we see better results in the second year, with good agreement between the observed and modeled ML depth and SST. However, at the end of the summer and during the winter of 1989, the simulated ML is still underestimated, particularly around day 400 and day 750. The model SST also cools faster than observed (Figure 4).

The absence of diffusion does not greatly influence the depth of the simulated ML over the two years. Indeed, somewhat better correlation with Station 27 data is observed, in the absence of diffusion, particularly at the beginning of the simulation. The ML depth computed with no diffusion is shallower than that for the diffusion case. However, the thinner mixed layer also produces an increased SST (Figure 4) which is too high. As we

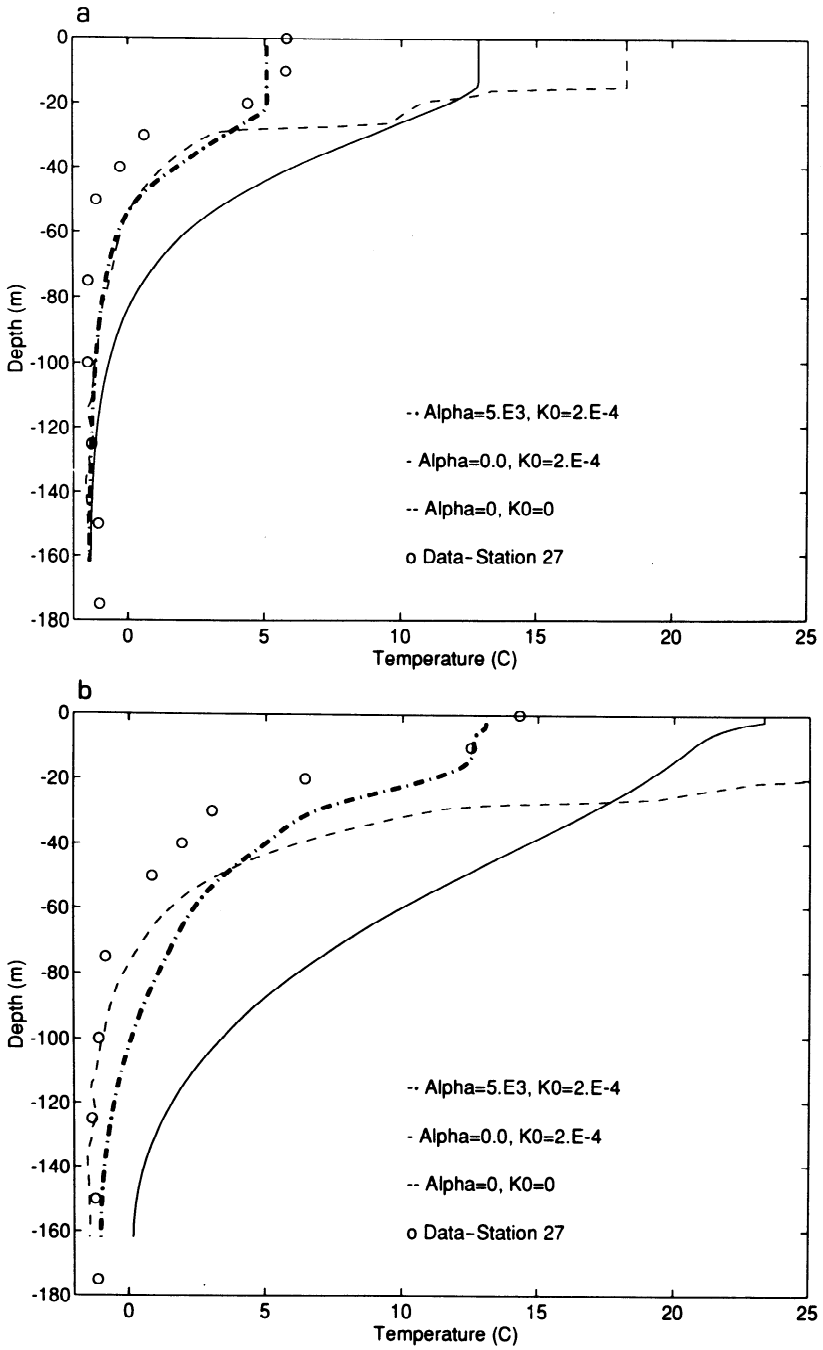

Figure 5. Vertical profiles of temperature (in degrees Celsius) for 6 days of simulated period for different values of α and k_o in equation (4): (a) day 153 (June 1, 1988), (b) day 239 (August 26, 1988), (c) day 421 (March 24, 1989), (d) day 497 (May 13, 1989), (e) day 616 (September 7, 1989), and (f) day 762 (February 10, 1990). Station 27 data are plotted with open circles, the no diffusion case with a dashed line, constant diffusivity with a solid line, and the depth dependent diffusivity with a heavy dot-dashed line.

shall see later, without diffusion there is too much heat in the water column.

4.3. Influence of Salinity

In the second series of simulations, we tested the influence of salinity upon the diffusion model. Effects of the different salinity data sets were investigated by including (1) sea surface salinity (SSS) and (2) monthly mean profiles of salinity from Station 27. Salinity is thus allowed to evolve in these model runs.

4.3.1. Response to sea surface salinity. The inclusion of sea surface salinity corresponds to a surface forcing which accounts for the salinity variation due to melting ice [*Mertz et al.*, 1993]. This forcing term replaces the evaporation-precipitation term in equation (3). Its influence is negligible according to Figure 7, in

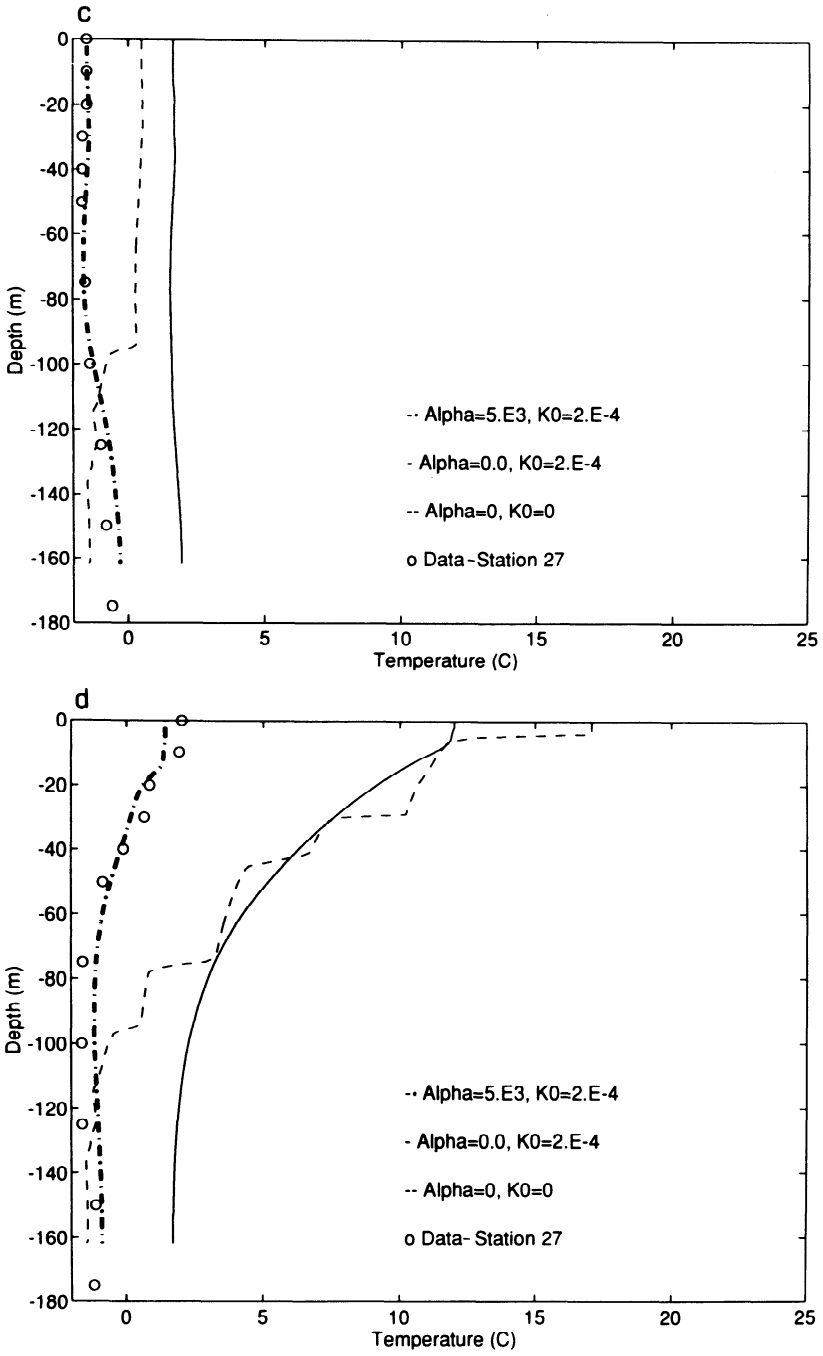

Figure 5. (continued)

which results for SST are presented. Analyses of temperature profiles over the two years (Figure 8) yields similar results, except in winter. A weak influence is observed at the beginning (day 350) and at the end of the 1988 winter (day 497). The temperature profile on day 350 highlights a warm water mass just beneath the mixed layer shallower than the no salinity case. This subsurface temperature maximum results from the rising of the mixed layer due to a density decrease in the upper layer. As mentioned above (see section 3), low water temperature in winter modifies the relative importance of salinity in density computation. A salinity decrease at depth has a weak influence, since the shallowing mixed layer prevents mixing processes from reaching deep layers. Diffusion through the bottom of the ML is not sufficient to allow a strong upward flux of heat. This warm water mass disappeared by the end of the winter because of the deepening of the ML (wind stress enhancement at the surface) which homogenizes the water column. However, by the next winter this subsurface temperature maximum reforms (Figure 8c).

4.3.2. Response to salinity profiles. In this run, we integrated monthly mean data profiles on the first day of each month to reproduce the seasonal cycle of salinity. This implementation was carried out to force the model to account for the change in the vertical profile of density, which depends strongly on salinity. This integration did not modify the SST over the two years,

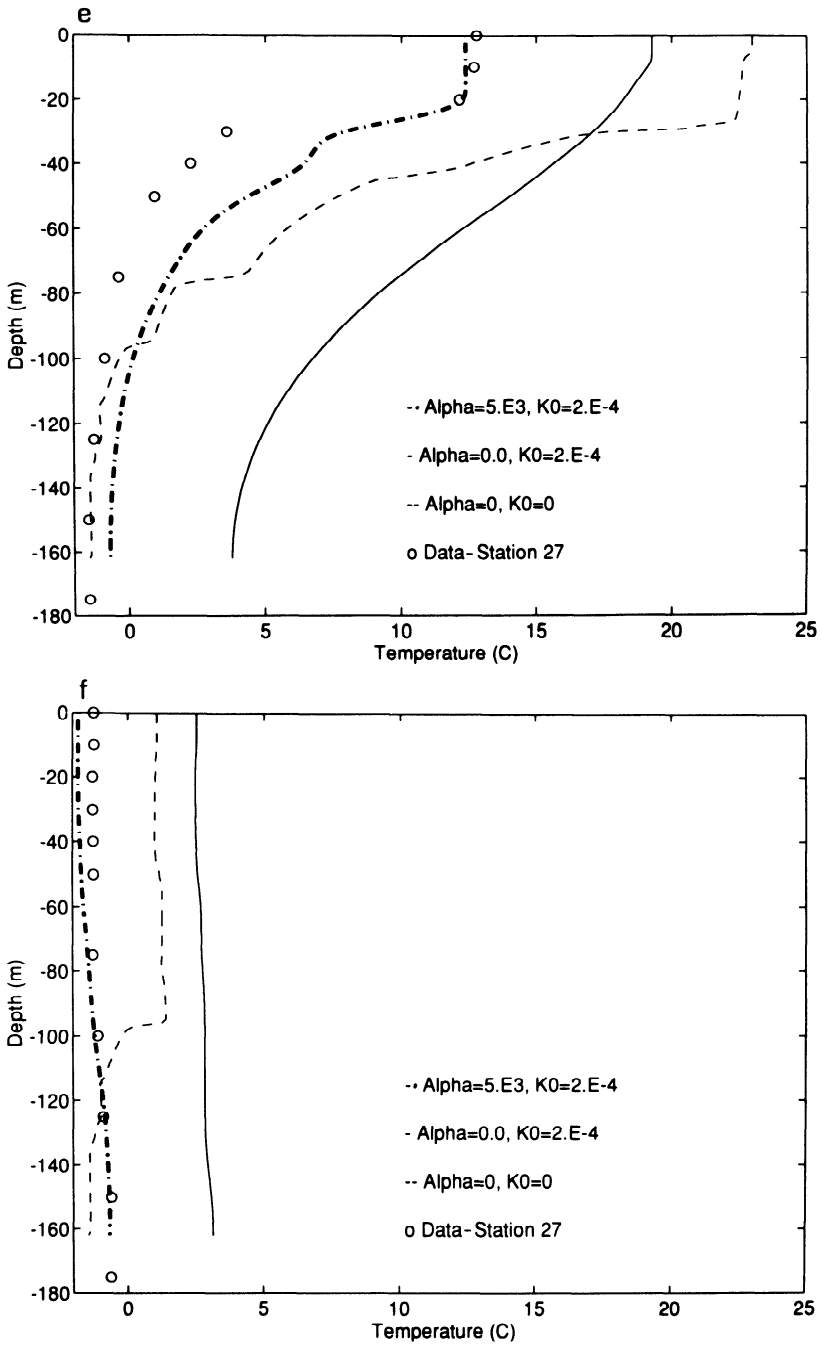

Figure 5. (continued)

with only small variations observed in the temperature profiles (Figure 8). Once again, a subsurface temperature maximum forms, but it is much less intense. The weaker effect is a consequence of the deepening of the ML due to the enhanced influence of low salinity in the upper layer.

4.4. Summary of Results

Temperature contours observed (Figure 9a) and modeled (Figure 9b) show good overall agreement. The model run used in this comparison is the case using variable diffusion but with no assimilation of salinity. Although this model produces good overall correlations, it does underestimate the ML depth during the winter. Weak stratification in the winter, which makes it difficult to determine the ML depth, may be the cause of the observed wintertime discrepancy in the ML depth.

Data from a thermistor chain mooring inside Conception Bay (Figure 1) correlate well with the model results (Figure 10), although there are some discrepancies (e.g., around day 230), providing further support for the model results. The thermistor chain data show variability at 2-10 days that is probably due to the wind-forced response since this mooring was within an internal Rossby radius of the coastline [*deYoung et*

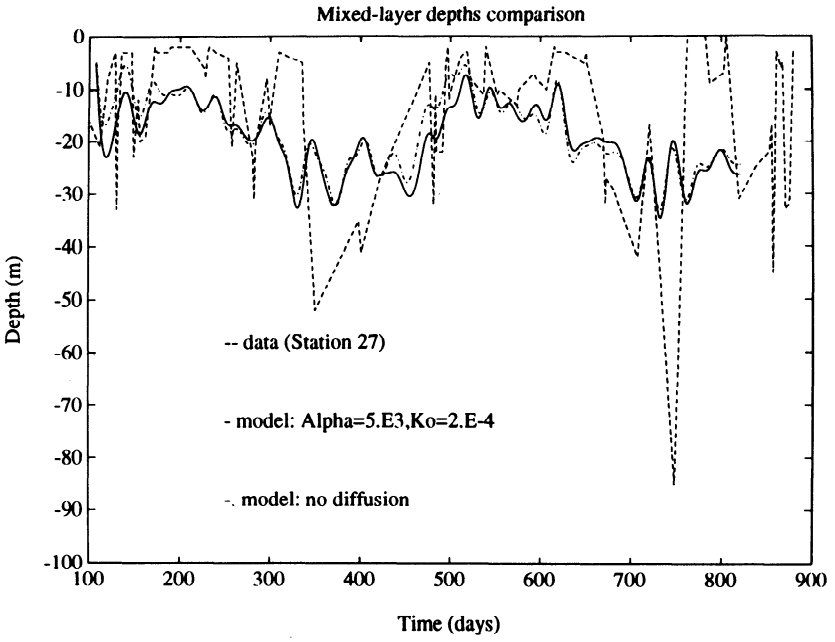

Figure 6. Comparison between observed and simulated mixed layer depth over the simulation period (1988-1989). The mixed layer depth is shown for different values of α and k_o in equation (4). Station 27 data are plotted with a dashed line, no diffusion with a dot-dashed line, and depth dependent diffusivity with a solid line.

al., 1993a]. At 27 m depth, the model tracks the observed data well (Figure 10a), except that the observed temperature is lower during the summer. The summer temperature differences are probably because the model ML depth does not reach reach 27 m. About day 240, temperature at 27 m drops to ~5°C because of a shallowing of the ML. This is confirmed by the increase of SST at the same time. At 77 m, model temperature is higher than observed between day 100 and day 180, which agrees well with the previous observations of the ML depth (Figure 6). During the summer, the simulated ML is deeper than observed upper layer, and

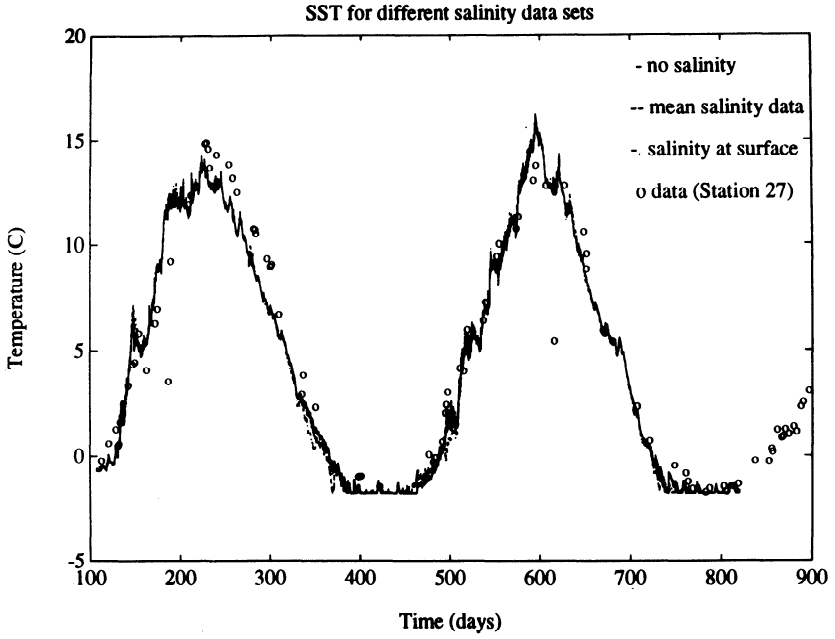

Figure 7. Time evolution of simulated sea surface temperature over the two years (1988-1989) for different salinity data sets: sea surface salinity (SSS), mean salinity profiles, and no salinity data excepted initial data. Station 27 data are plotted with open circles, the no diffusion case with a dot-dashed line, constant diffusivity with a dashed line, and the depth dependent diffusivity with a solid line.

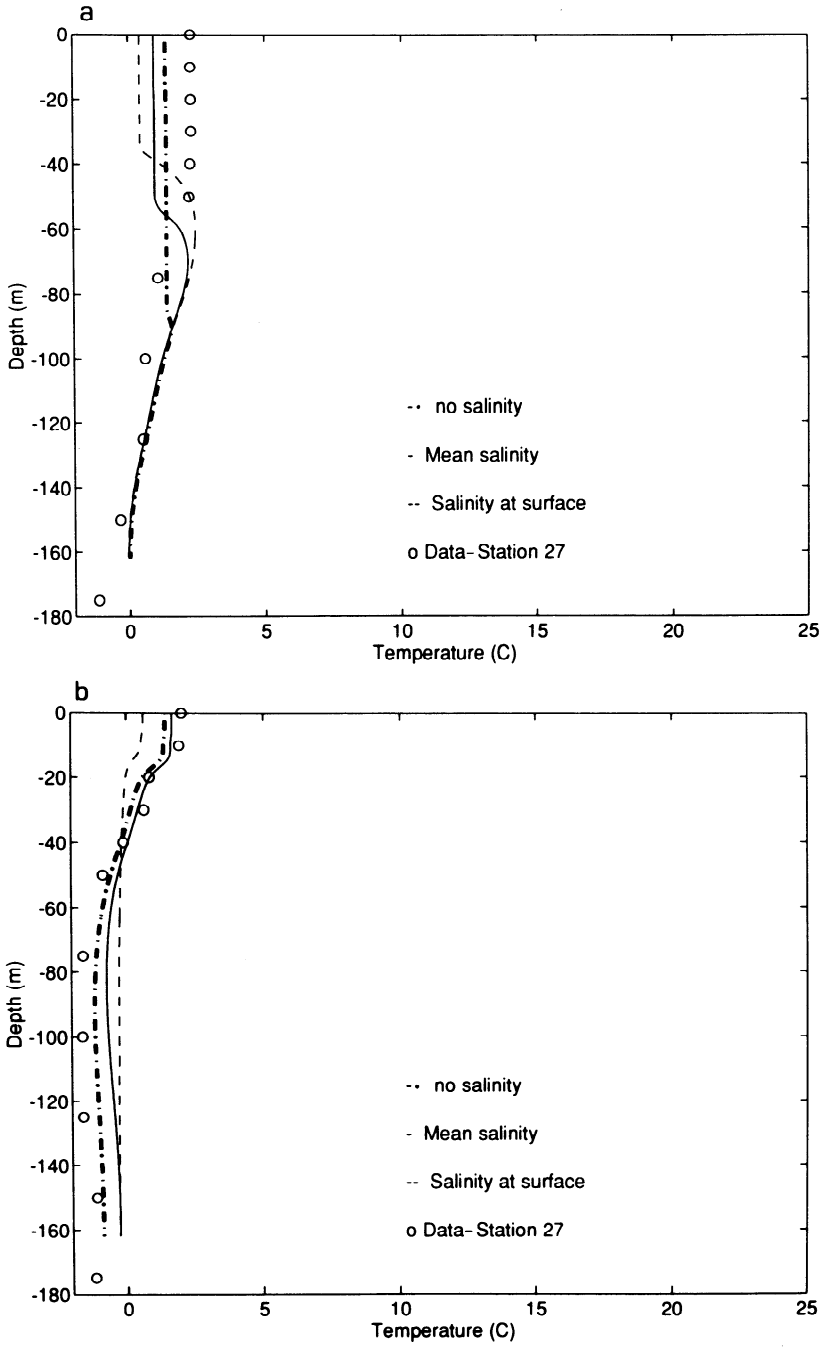

Figure 8. Vertical profiles of temperature (in degrees Celsius) during the simulation period for different salinity data sets: (a) day 350 (December 15, 1988), (b) day 497 (May 13, 1989), and (c) day 762 (February 10, 1990). Station 27 data are plotted with open circles, the model with no salinity with a heavy dot-dashed line, the model with mean monthly salinity with a dashed line, and surface salinity only with a solid line.

thus the ML heat may influence temperature at 77 m through diffusion. Heat content of the water column shows a similar annual cycle, but the amplitude of the variation is not proportional to the time evolution of the upper layer temperature (Figure 11). With no diffusion, the highest SST is obtained although the heat content is lower than the run using a constant diffusion. The constant diffusion over the depth induces a downward heat flux from the ML to deep layers which decreases the surface temperature. Thus the air-sea temperature increases, permitting a greater heat input from atmosphere to ocean. In the last case, where the diffusion coefficient depends on depth, the water column acquires a structure which reduces the input of heat from the atmosphere, and the modeled temperature at different depths matches fairly well the data at Station 27 (Figure 4 and Figures 10a and 10b).

In Figure 11, the difference in heat content is observed

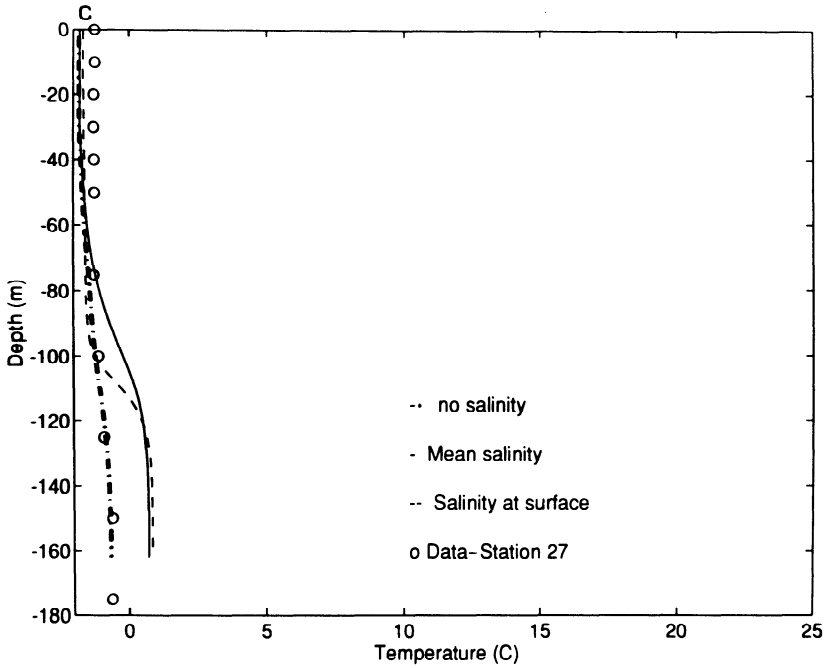

Figure 8. (continued)

during the summer period of the two years. The discrepancy between day 210 and 250 in Figures 10a and 10b is matched by the discrepancies observed in Figure 11. In Figure 11, there is a difference in heat content during the summer period of the two years. This deviation corresponds to the period when surface salinity reaches a minimum because of the freshwater flux driven by melting sea ice [*Petrie et al.*, 1992]. The absence of advection in this model is probably the reason for the lack of agreement during this period. It is, however, interesting that even when we relax salinity in the model to the observed salinity we do not get good agreement during this period. This suggests that there is a net heat flux during this period, something not found by *Petrie et al.* [1992] from their fitting of a diffusion equation to the data.

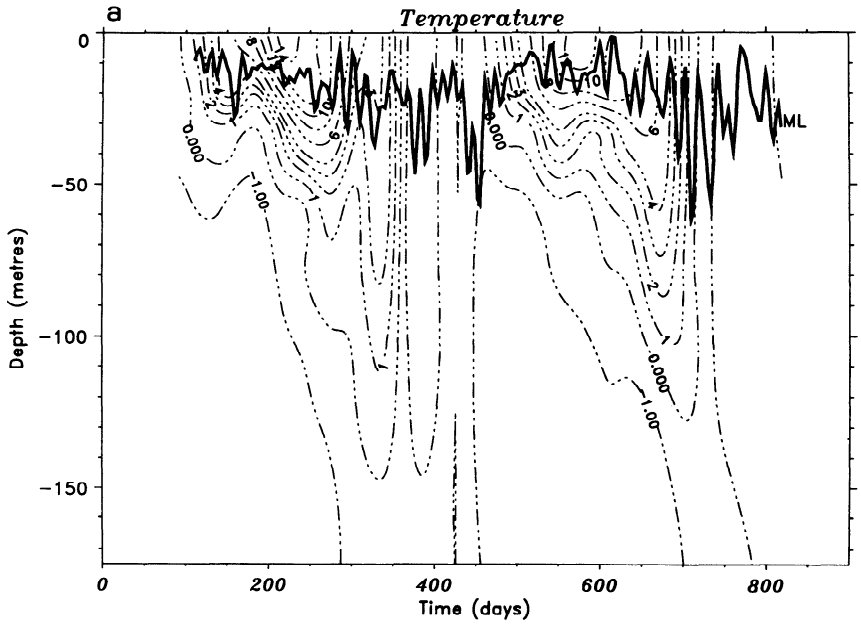

Figure 9. (a) Overlay of computed mixed layer depth (solid lines) and contour lines of observed temperature at Station 27 (dashed contours). Model results were filtered to remove energy at periods below a day. (b) Model temperature contours (in degrees Celsius) over 1988 and 1989 for the model with depth dependent diffusivity and only initial salinity.

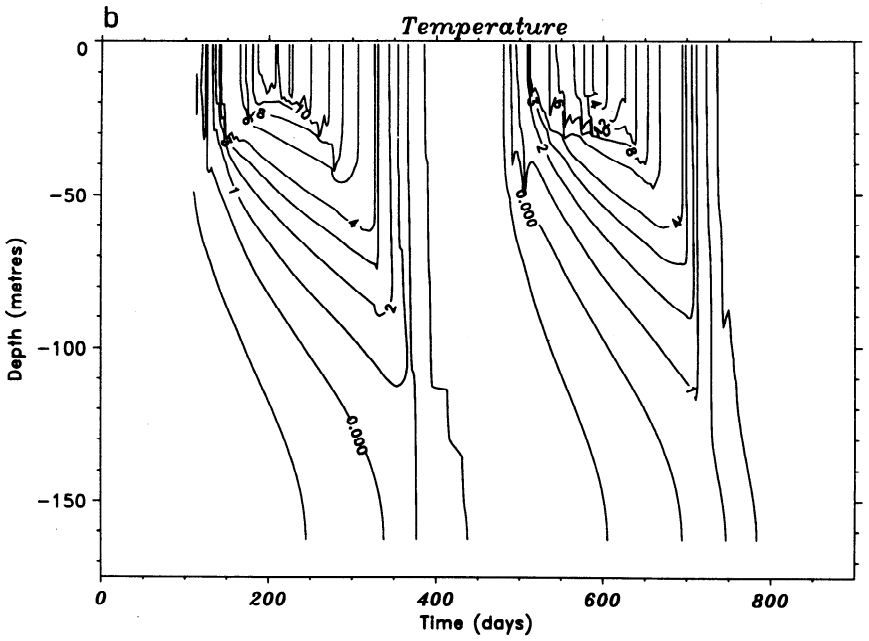

Figure 9. (continued)

5. Discussion and Conclusions

In this study, two modifications to the PWP model [*Price et al.*, 1986] have been investigated in order to compare results of the simulations with data collected at Station 27 offshore of St John's, Newfoundland. We have added salinity to the calculation of σ_t and vertical diffusion to the model, changes which produced much improved model simulations. We tested the sensitivity of the model to different parameterizations of the vertical diffusivity, using as a model the work of *Umoh* [1992], whose parameterization of vertical diffusivity depends upon the vertical profile of the Brünt-Väisälä frequency. Three cases of diffusion coefficients were analyzed.

No diffusion. This is similar to the initial PWP model in which the density jump at the bottom of the mixed layer is reduced by the existence of a transition layer. SST obtained from this simulation did

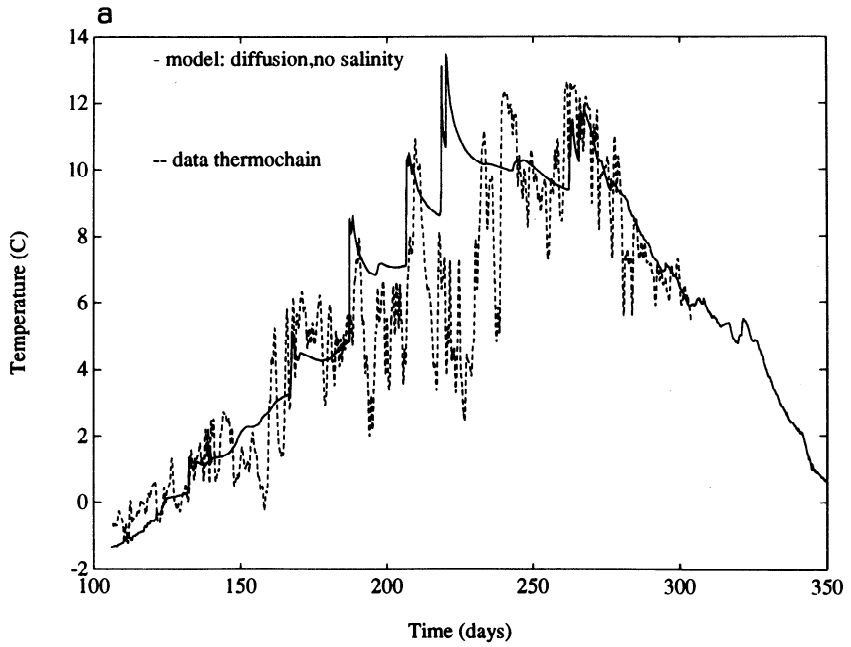

Figure 10. Plots of thermistor chain data (dashed line) for 1989 from inside Conception Bay versus temperature output of the model (solid line) at (a) 27 m and (b) 77 m depth. For this model run, depth dependent diffusivity and only initial salinity are applied.

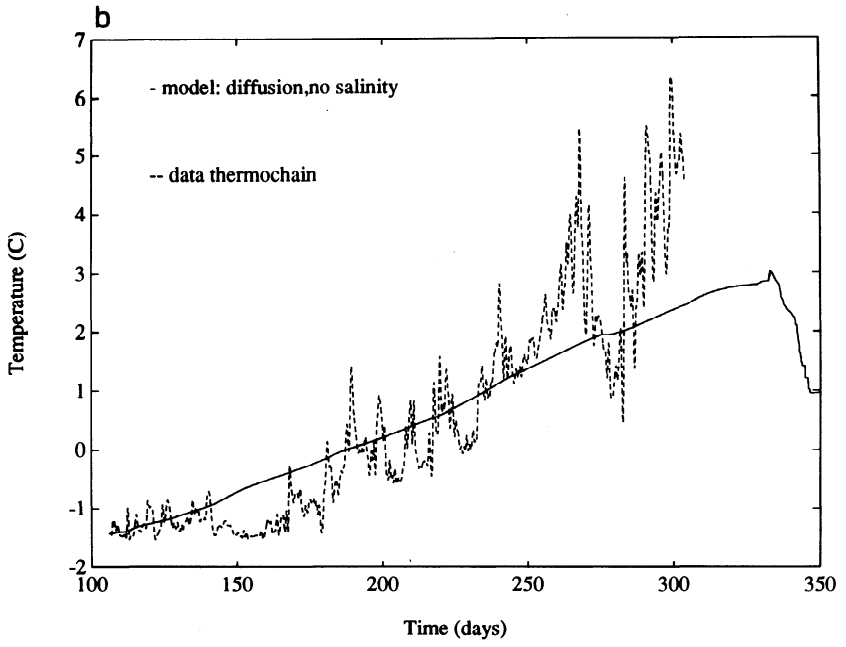

Figure 10. (continued)

not match Station 27 observations, although the mixed layer showed good agreement with the data. In the absence of diffusion, too much heat was retained in the water column.

Constant diffusion over depth. SST obtained from this simulation showed some improvement in the ML temperature over the no-diffusion case. However, with the improved surface temperature the heat content of the whole water column increases with far too much heat at depth.

Depth dependent diffusion. SST results from these simulations agree well with data. Modeled ML depth is not improved strongly during this simulation; agreement with the observed mixed layer depth is reasonable for all the model runs. Only in winter, when the depth is underestimated, is the agreement poor. Other models also exhibit this shortcoming [*Martin*, 1985].

The location of the study area suggested the importance of salinity data in modeling of the seasonal ML depth and SST evolution. The results obtained by including salinity data as a constraint did not show

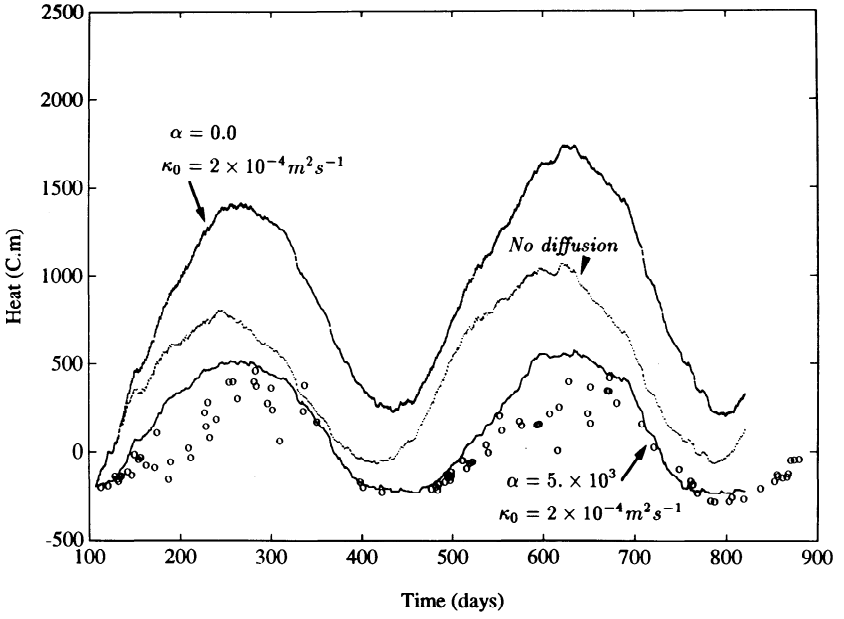

Figure 11. Time evolution of heat content for the whole water column for different values of α and k_o, different forms of vertical diffusivity. Station 27 data are plotted with open circles, the no diffusion case, the constant diffusivity, and the depth dependent diffusivity curves are labeled.

any improvement in agreement with the observations. On the contrary, adding salinity produced a subsurface temperature maximum not observed in the data. There is, however, an indirect effect of salinity, through N^2, which influences κ_v each month. The agreement that we find suggests that the most important influence of salinity can be taken into account through the vertical diffusivity.

The two primary results of our work are that (1) for a long-term simulation, inclusion of diffusion in the PWP bulk model is necessary and (2) the assimilation of salinity does not improve the model results.

This work is the first step in a project to investigate the response of phytoplankton to episodic upwellings in Conception Bay. *Marra and Ho* [1993] used the PWP model to simulate the spring bloom in the North Atlantic and obtained good results on a short timescale. In our case, a long-term study is necessary to take into account successive upwelling events. This one-dimensional model encourages us to develop a three-dimensional model using this basic approach to apply to upwelling in the bay [*deYoung et al.*, 1993a]. The modified PWP model provides good results for the long-term simulations needed.

Acknowledgments. The authors would like to thank R. Greatbatch for early encouragement of this work, and P. Fardy, who provided help with the plotting of some of the figures. We thank two reviewers for their comments on the original version of this manuscript. T. M. would like to acknowledge NSERC operating grant support from D. Schneider and the partial support of a fellowship from the University of Liege (Belgium). B. deY. acknowledges the support of an NSERC operating grant and the Ocean Production Enhancement Network (OPEN).

References

Denman, K. L., A time dependent model of the upper ocean, *J. Phys. Oceanogr., 3*, 173-184, 1973.

Dera, J., *Marine Physics*, 516 pp., Elsevier, New York, 1992.

deYoung, B., and S. Pond, The deepwater exchange cycle in Indian Arm, British Columbia, *Estuarine Coastal Shelf Sci., 26*, 285-308, 1988.

deYoung, B., T. Otterson, and R. Greatbatch, The local and non-local response of Conception Bay to wind forcing, *J. Phys. Oceanogr., 23*, 2636-2649, 1993a.

deYoung, B., R. Greatbatch, and K. Forward, A diagnostic coastal circulation model with application to Conception Bay, Newfoundland, *J. Phys. Oceanogr., 23*, 2617-2635, 1993b.

Gargett, A. E., Vertical diffusion in the ocean interior, *J. Mar. Res., 42*, 359-393, 1984.

Gaspar, P., Modelling the seasonal cycle of the upper ocean, *J. Phys. Oceanogr., 18*, 161-180, 1988.

Gill, A., *Atmosphere-Ocean Dynamics*, 662 pp., Academic, San Diego, Calif., 1982.

Jones, J. H., Vertical mixing in the Equatorial Undercurrent, *J. Phys. Oceanogr., 3*, 286-296, 1973.

Häkkinen, S., and D. J. Cavalieri, A study of oceanic surface heat fluxes in the Greenland, Norwegian, and Barents seas, *J. Geophs. Res., 94*, 6145-6157, 1989.

Krauss, E. B., *Atmosphere-Ocean Interactions*, 275 pp., Clarendon, Oxford, 1972.

Krauss, E. B., and J. S. Turner, A one-dimensional model of the seasonal thermocline, 2, The general theory and its consequences, *Tellus, 19*, 98-105, 1967.

Large, W. G., and S. Pond, Open ocean momentum flux measurements in moderate to strong winds, *J. Phys. Oceanogr., 11*, 324-336, 1981.

Largier, J. L., Deep surface mixed layers on the continental shelf, *Cont. Shelf Res., 10*, 759-776, 1991.

Marra, J., and C. Ho, Initiation of the spring bloom in the northeast Atlantic (47°N, 20°): A numerical simulation, *Deep Sea Res., 40*, 55-73, 1993.

Martin, P. J., Simulation of the mixed layer at OWS November and Papa with several models, *J. Geophys. Res., 90*, 903-916, 1985.

Mertz, G., S. Narayanan, and J. Helbig, The freshwater transport of the Labrador Current, *Atmos. Ocean, 31*, 281-295, 1993.

Munk, W. H., and E. R. Anderson, Notes on a theory of the thermocline, *J. Mar. Res., 7*, 276-295, 1948.

Nihoul, J. C. J., A three-dimensional general marine circulation model in a remote sensing perspective, *Ann. Geophys., 2*, 433-443, 1984.

Niiler, P. P., Deepening of the wind-mixed layer, *J. Mar. Res., 33*, 405-422, 1975.

Niiler, P. P. and E. B. Krauss, One dimensional models, in *Modelling and Prediction of the Upper Layers of the Ocean*, edited by E. B. Krauss, pp. 143-172, Pergamon, New York, 1977.

Pacanowski, R. C., and S. G. H. Philander, Parameterization of vertical mixing in numerical models of tropical oceans, *J. Phys. Oceanogr., 11*, 1443-1451, 1981.

Parkinson, C. L. and W. M. Washington, A large-scale numerical model of sea ice, *J. Geophy. Res., 84*, 311-337, 1979.

Paulson, C. A., and J. J. Simpson, Irradiance measurements in the upper ocean, *J. Phys. Oceanogr., 7*, 952-956, 1977.

Petrie, B., J. W. Loder, S. Akenhead, and J. Lazier, Temperature and salinity variability on the eastern Newfoundland shelf: The annual harmonic, *Atmos. Ocean, 29*, 14-36, 1991.

Petrie, B., J. W. Loder, S. Akenhead, and J. Lazier, Temperature and salinity variability on the eastern Newfoundland shelf: The residual field, *Atmos. Ocean, 30*, 120-139, 1992.

Price, J. F., C. N. K. Mooers, and J. C. van Leer, Observation and simulation of storm-induced mixed-layer deepening, *J. Phys. Oceanogr., 8*, 582-599, 1978.

Price, J. F., R. A. Weller, and R. Pinkel, Diurnal cycling: Observations and models of the upper ocean response to diurnal heating, cooling and wind mixing, *J. Geophys. Res., 91*, 8411-8427, 1986.

Robinson, A. R., An investigation into the wind as the cause of the Equatorial Undercurrent, *J. Mar. Res., 24*, 179-204, 1966.

Stigebrandt, A., Vertical diffusion driven by internal waves in a sill fjord, *J. Phys. Oceanogr., 6*, 486-495, 1976.

Umoh, J., Seasonal and interannual variability of sea temperature and surface heat fluxes in the northwest Atlantic, Ph.D. thesis, 237 pp., Dalhousie Univ., Halifax, Nova Scotia, Canada, 1992.

Yamada, T., and G. L. Mellor, A simulation of the Wangara atmospheric boundary layer, *J. Atmos. Sci., 31*, 1297-1307, 1974.

B. deYoung and T. Mathieu, Department of Physics, Memorial University of Newfoundland, St. John's, Newfoundland, Canada A1B 3X7. (email: bdeyoung@crosby.physics.mun.ca)

(Received August 10, 1993; revised March 15, 1994; accepted May 13, 1994.)